A

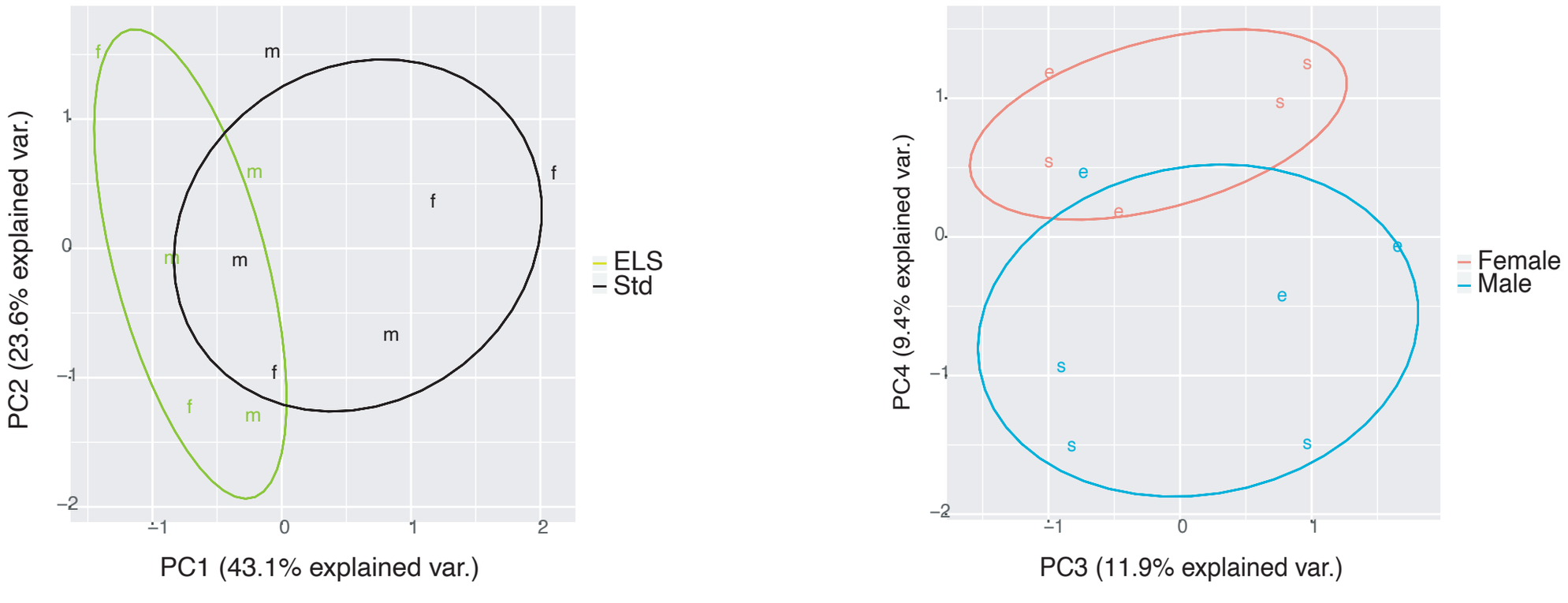

B

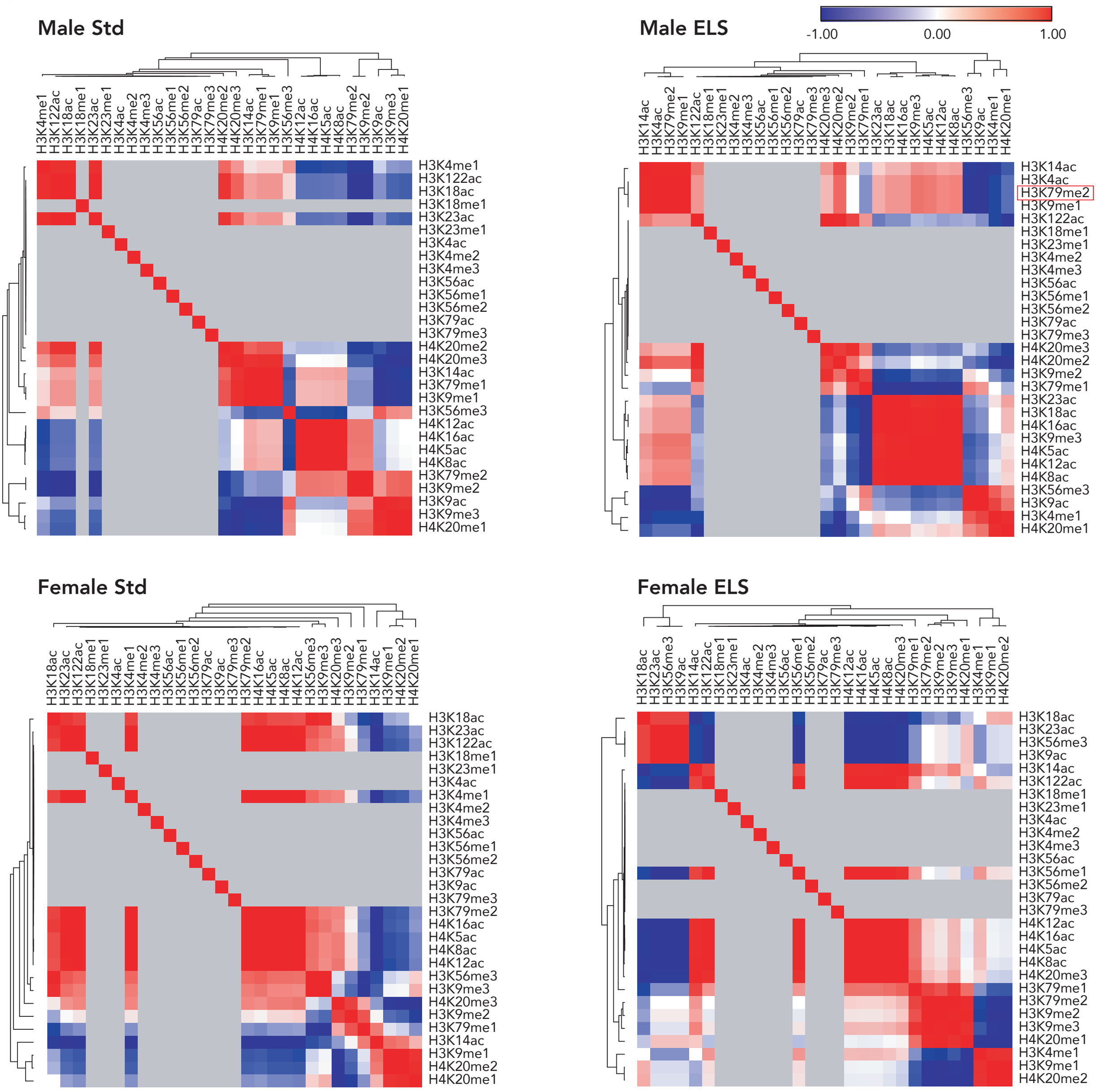

C

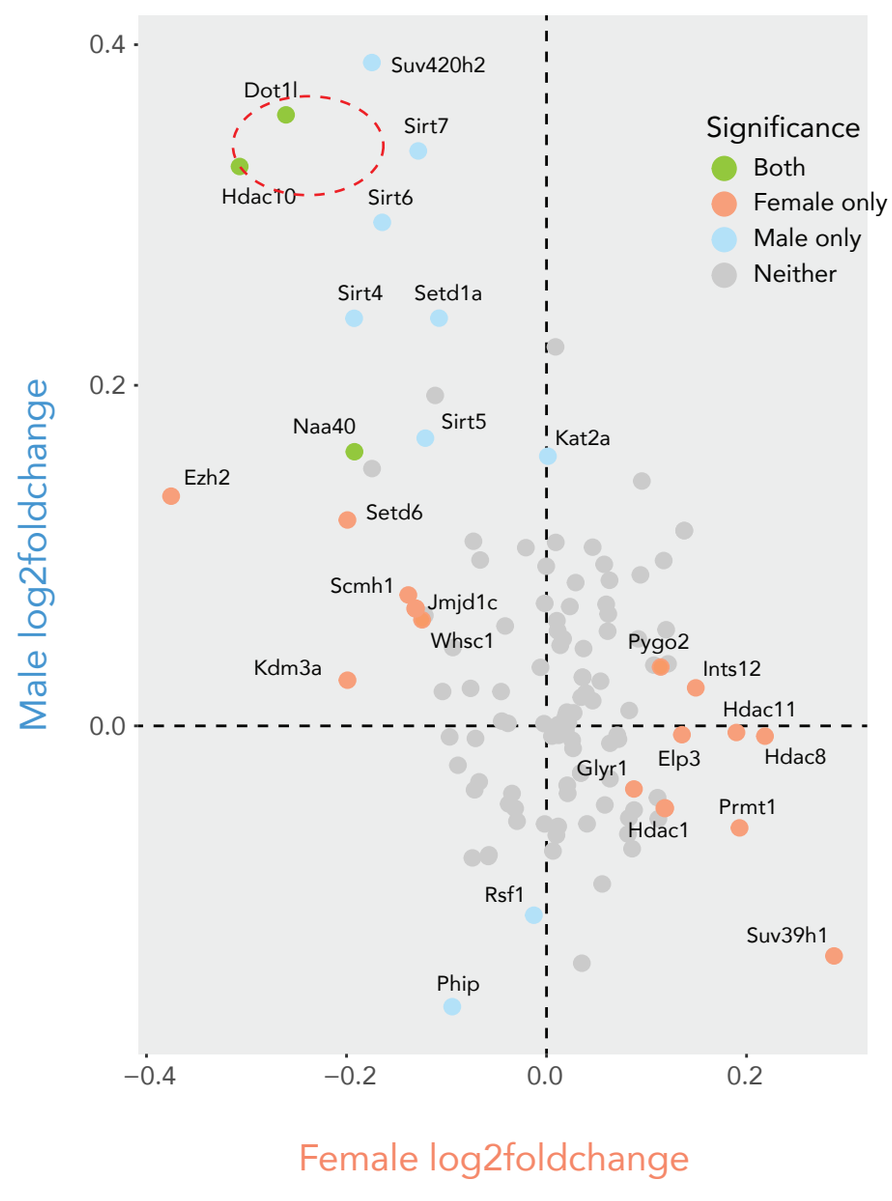

Figure S1. Mass spectrometry data principal components and networks of correlated marks

(A) Principal component graphs; concentration ellipses determined by means and covariance of groups. Panel A shows PC1/PC2 and Panel B shows PC3/PC4

(B) Correlation by Euclidean distance of histone modifications within group

(C) Fold change of epigenetic writers and erasers in male and female post-ELS NAc datasets from Peña et al, 2019

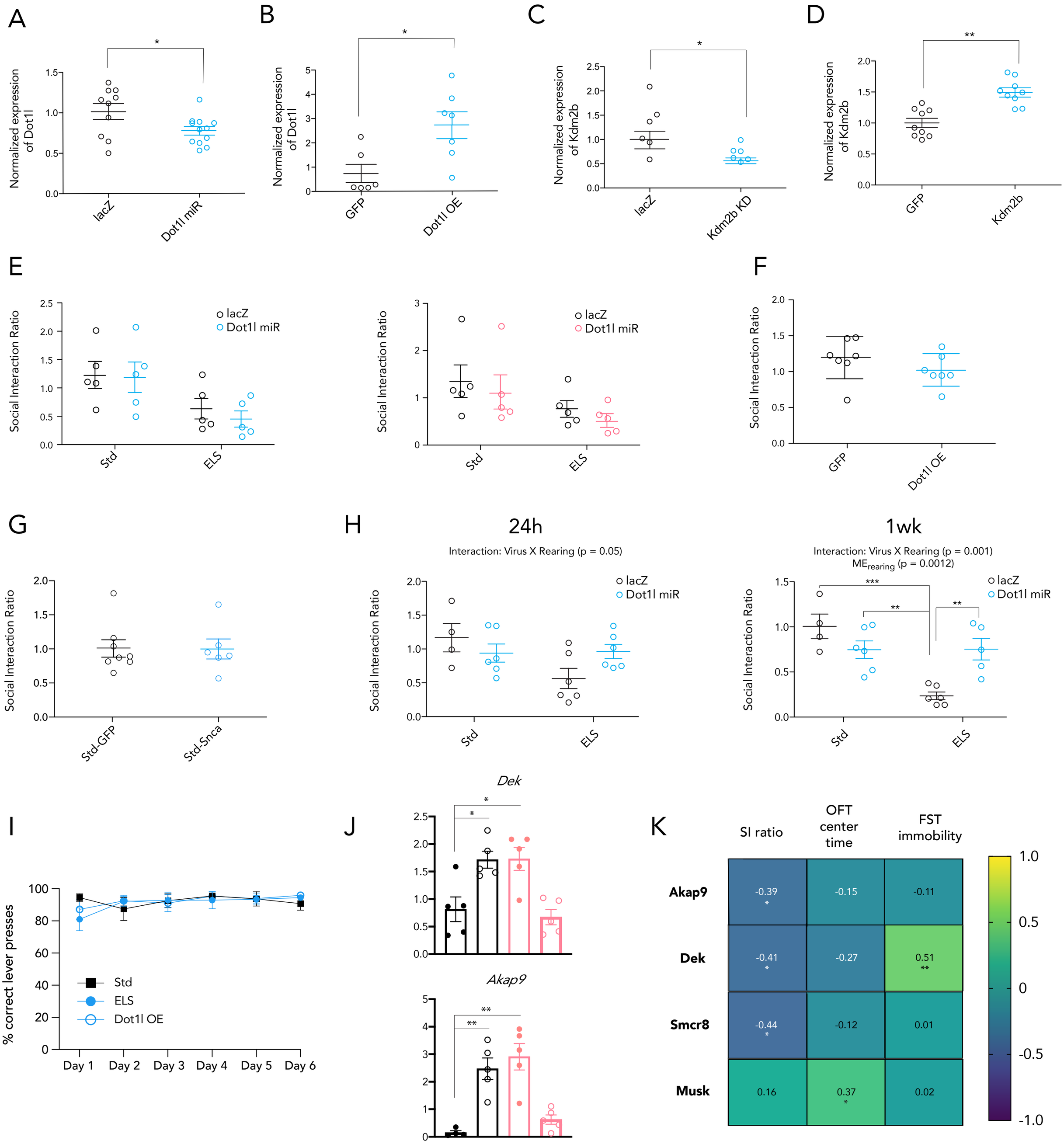

Figure S2. Viral validation and behavioral specificity

(A) qPCR of *Dot1l* in whole NAc tissue following *Dot1l* knockdown using a cell type-specific HSV
(B) qPCR of *Dot1l* in whole NAc tissue following *Dot1l* overexpression using a cell type-specific HSV
(C) qPCR of *Kdm2b* in whole NAc tissue following *Kdm2b* knockdown using a cell type-specific HSV
(D) qPCR of *Kdm2b* in whole NAc tissue following *Kdm2b* overexpression using a cell type-specific HSV
(E) *Dot1l* knockdown in D1 MSNs of male and female mice does not produce social interaction deficits following social defeat
(F) *Dot1l* overexpression in D2 MSNs of the PFC does not produce social interaction deficits following social defeat
(G) *Snca* overexpression in D2 MSNs of the NAc does not produce social interaction deficits following social defeat
(H) Social interaction deficits are amplified over the week following social defeat
(I) Std, ELS, and animals with D2 MSN-specific *Dot1l* overexpression all acquire the initial task with equal accuracy
(J) qPCRs of whole NAc tissue from female ELS mice that underwent behavioral testing in Figure 3
(K) Correlation of male qPCRs with male behaviors from Figures 4 and 3, respectively

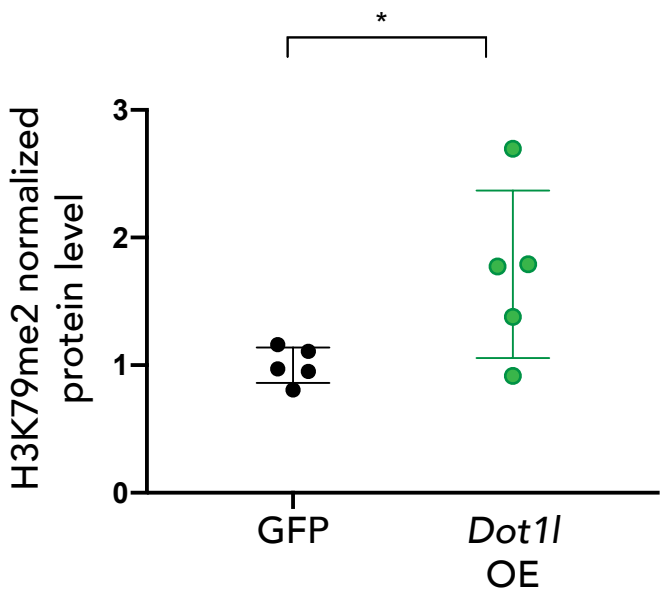

Figure S3. Whole tissue detection of H3K79me2 after D2 MSN-specific overexpression of *Dot1l*. Performed by ELISA.

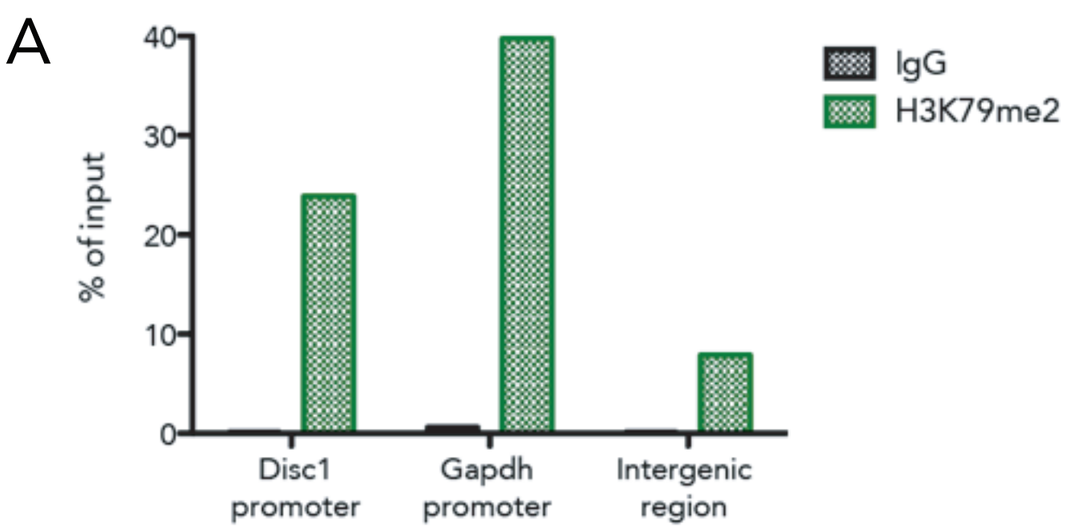

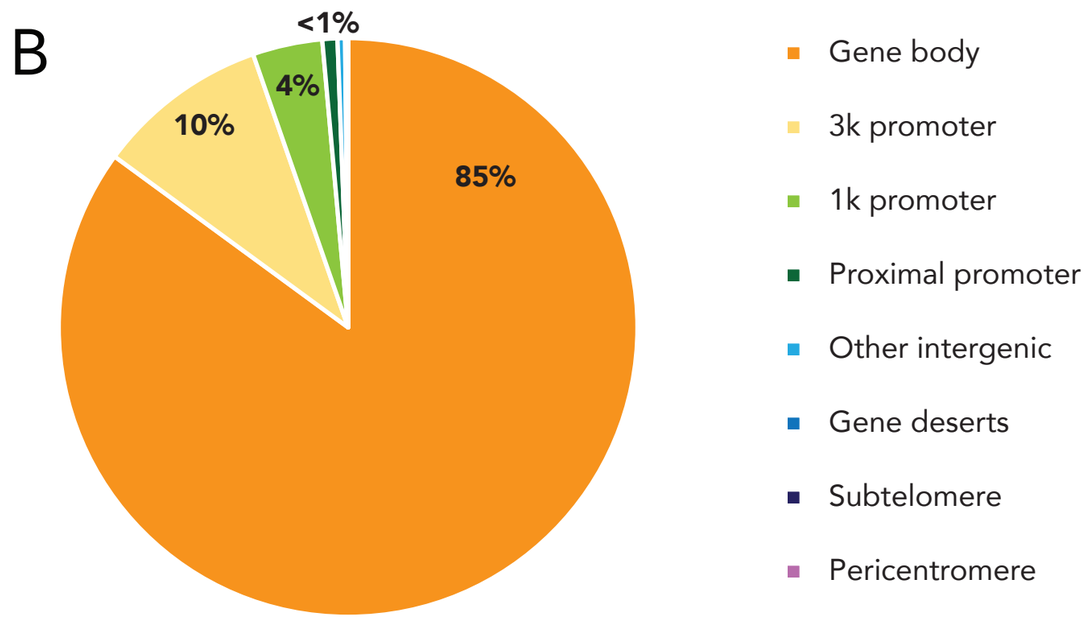

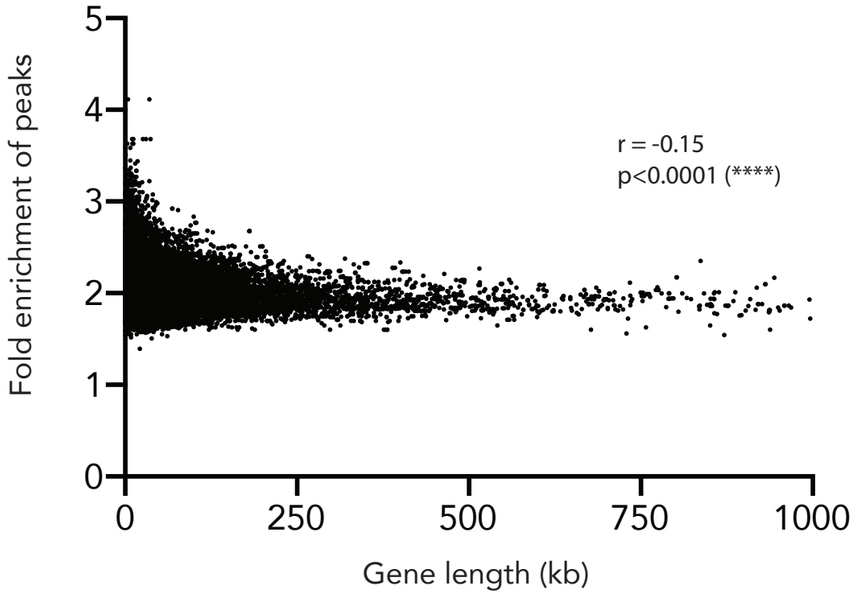

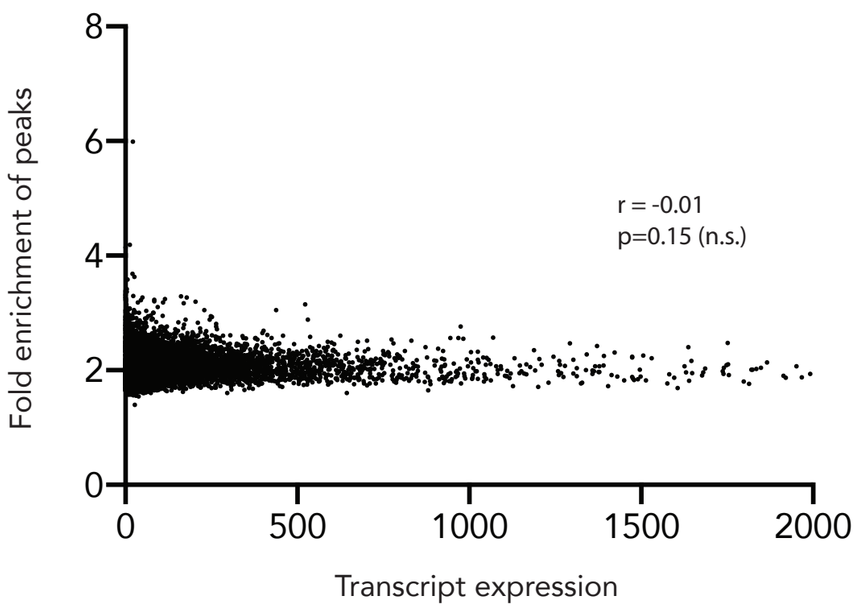

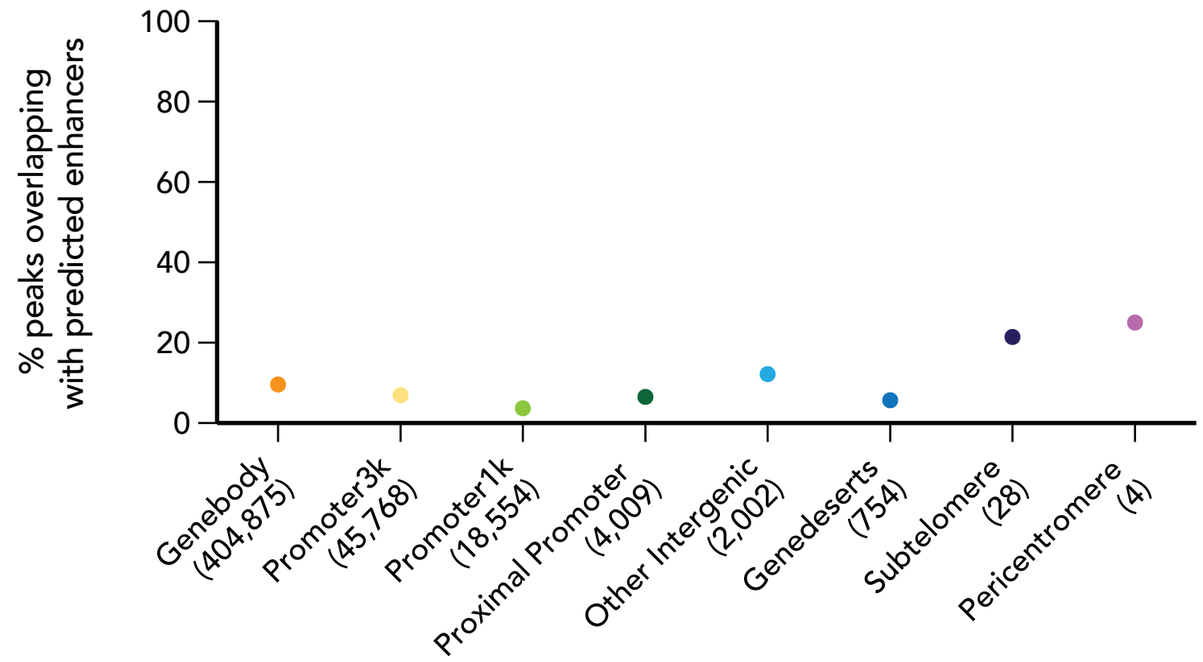

Figure S4. ChIP antibody, data quality, and baseline characteristics of H3K79me2 in NAc

(A) qPCR of DNA pulled down by IgG and H3K79me2 antibodies. Values represent percent of input.

(B) Distribution of H3K79me2 peaks in Std adult animals

(C) Fold enrichment of H3K79me2 peaks in Std adult animals compared to gene length and transcript expression (baseMean value in ELS vs Std DESeq2 comparison). r and p values from Pearson correlations.

(D) Percentage of H3K79me2 peaks in Std adult animals that overlap with enhancer loci predicetd in mouse NAc. No enrichment of these enhancer-overlapping peaks.

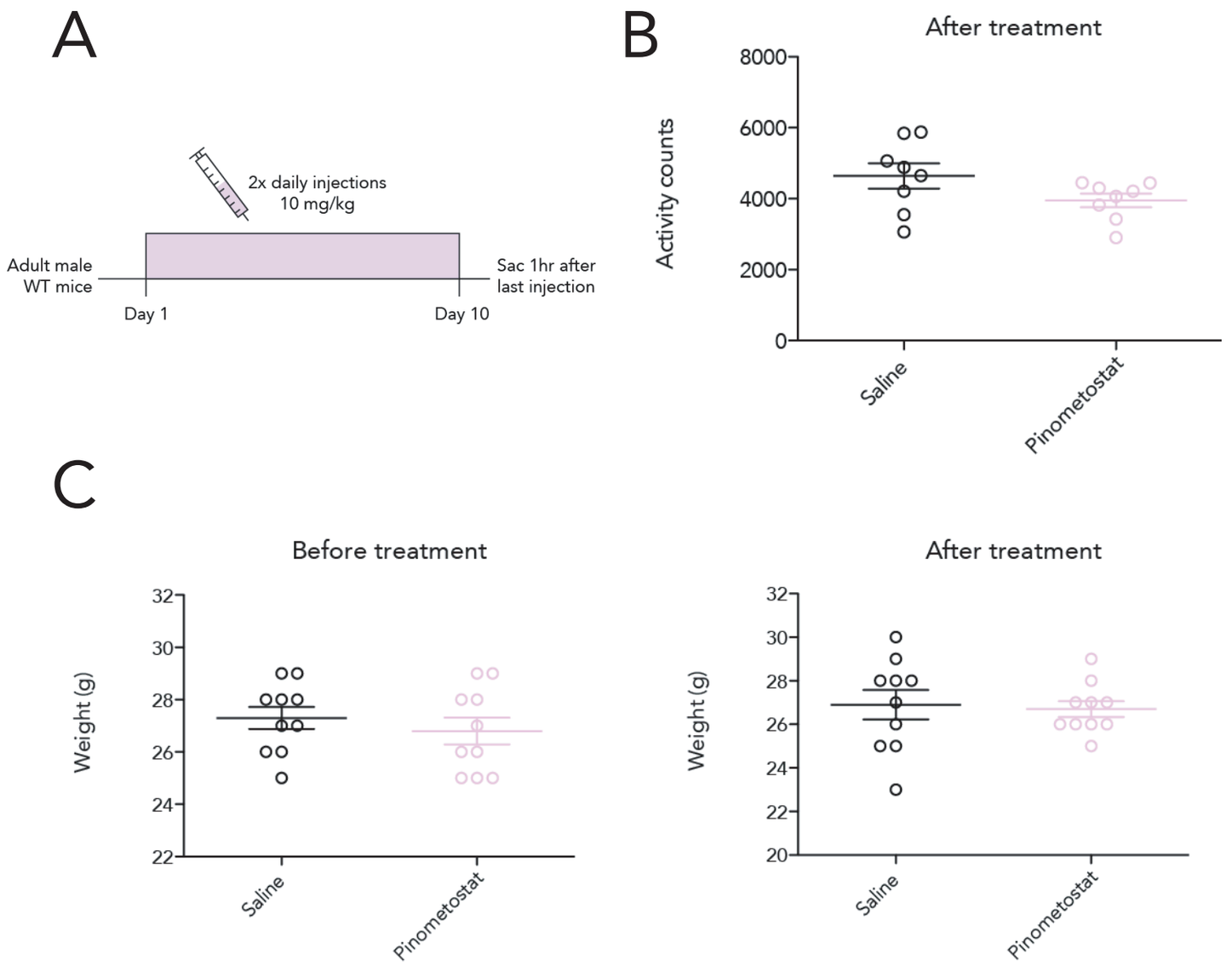

Figure S5. Pinometostat treatment does not alter locomotor activity or weight.

(A) Schematic of IP Pinometostat administration
(B) Locomotor activity after treatment with Pinometostat or saline. Measured in beam breaks.
(C) Weight of Pinometostat- and saline-treated animals

A

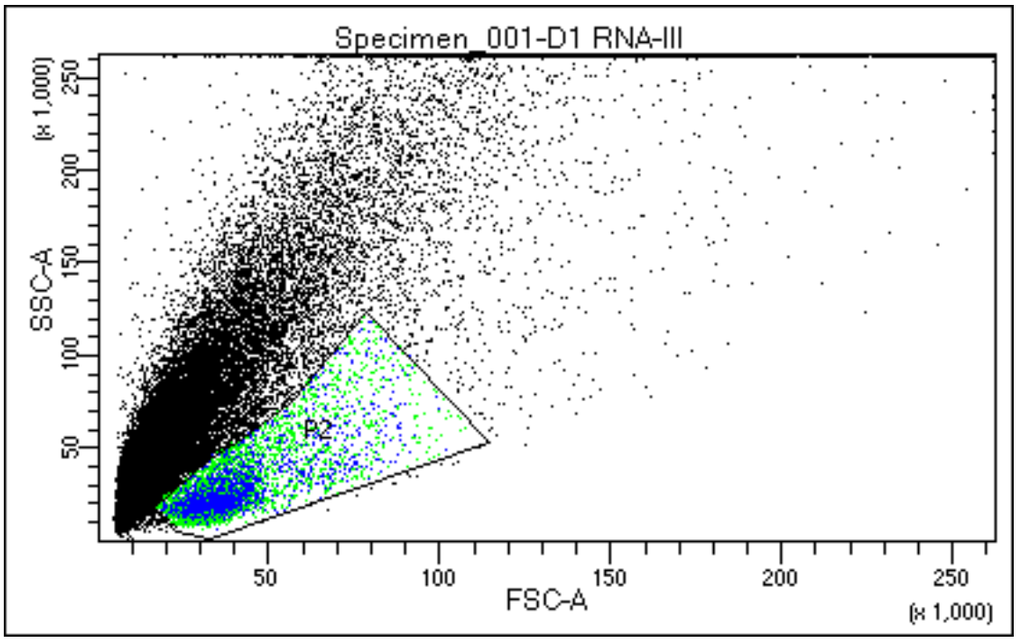

B

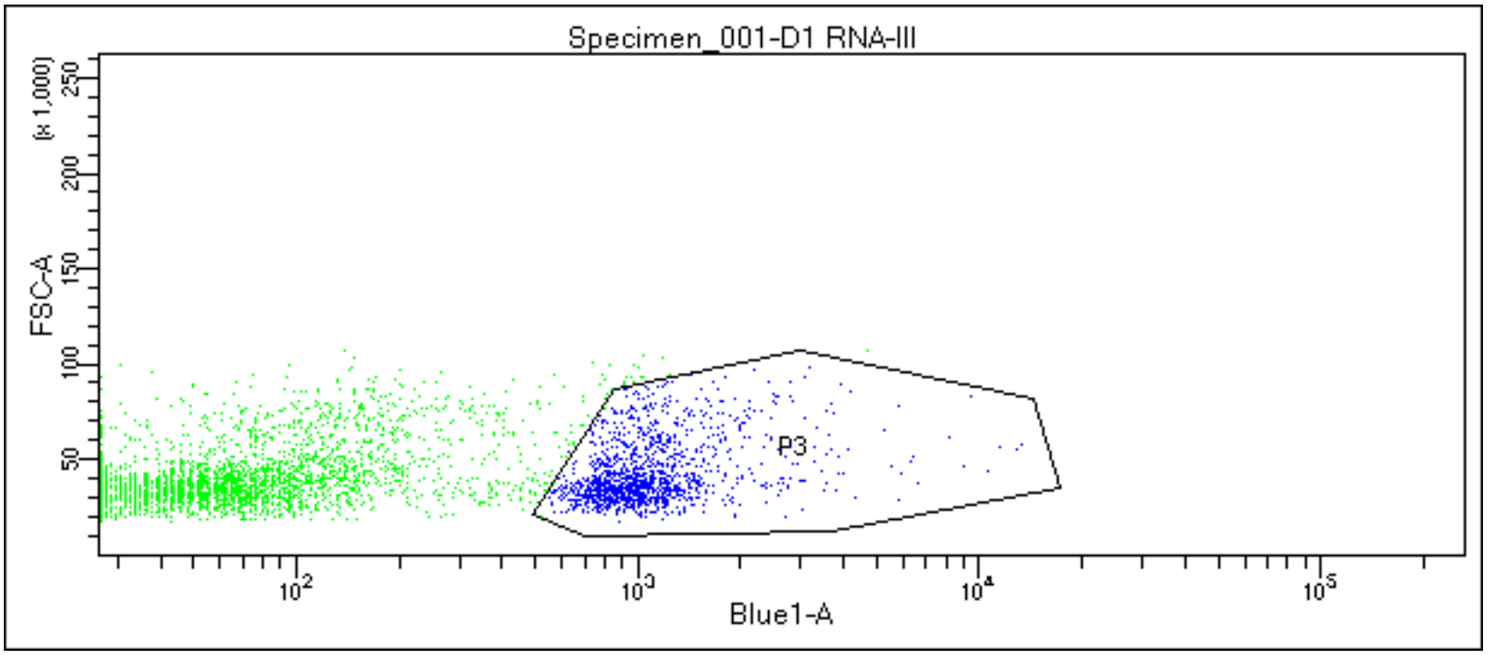

Figure S6. Representative gating for nuclear FACS

(A) First gate on FSC-A vs SSC-A retrieves nuclei (circled) as opposed to debris
(B) Second gate on FSC-A vs Blue1-A (FITC channel) separates transgenically labeled nuclei from wild-type nuclei